Modeling of Light Distribution in Tissue by

Monte Carlo Simulation

a thesis submitted in the partial fulfillment of the requirements for a degree of

Bachelor of Technology

in

Biotechnology

By: Priyanka

108BT021

Under the guidance of

Dr. Amitesh Kumar

Department of Biotechnology and Medical Engineering

National Institute of Technology

Rourkela, India

2012

National Institute of Technology, Rourkela

Certificate

This is to certify that the project entitled "Modeling of light distribution in tissue by Monte Carlo simulation" is submitted by Priyanka, student of Biotechnology branch of Department of Biotechnology and Medical Engineering, National Institute of Technology, Rourkela, for the degree of Bachelor of Technology is a record based on the results obtained in the bonafide research work carried out by her under my guidance and supervision.

To the best of my knowledge, the matter embodied in the project has not been submitted to any other University/Institute for the award of any degree or diploma.

Date:

Dr. Amitesh Kumar
Assistant Professor
Department of Biotechnology and Medical Engineering
National Institute of Technology
Rourkela-769008

ACKNOWLEDGEMENT

I avail this opportunity for extending my sincere appreciation and hearty gratitude to the guide Dr. Amitesh Kumar, Department of Biotechnology and Medical Engineering, National Institute of Technology, Rourkela for his invaluable academic support and professional guidance, regular encouragement and kind help at different stages of this project.

I would also like to express my gratitude towards my project companions and friends for helping me directly or indirectly in this project.

Finally, I am indebted to my parents and elder brothers for their patience, endurance, ceaseless, and moral support which made the completion of the project possible.

Date:

Priyanka

108BT021

Department of Biotechnology and Medical Engineering

National Institute of Technology, Rourkela

Odisha, India

CONTENTS

NOMENCLATURE

Symbol	Description	Unit
a	uniform irradiance beam radius	cm
A	the fractional density of incident light absorbed	$1/cm^3$
D	thickness of the tissues	cm
E_0	collimated irradiance	W/m^2
g	anisotropy factor of tissue	
n	refractive index of the tissue	
OD	Optical Depth	cm
P	power delivered	W
Q	delivered energy	J
r_{sc}	Fresnel surface reflectance	
R_r	escaping flux through front surface	$1/cm^2$
s	step size	cm
S_r	local density of power at r=(x, y, z)	W/cm^3
T_r	escaping flux through rear surface	$1/cm^2$
w	initial photon weight	
W_r	local density of energy deposition	J/cm^3
Greek		
δ	Penetration depth	cm
μ_a	absorption coefficien	cm^{-1}

μ_s	scattering coefficient	
μ_t	total attenuation coefficient	cm^{-1}
φ	Fluence	J/m^2
ψ	Fluence rate	W/m^2
θ	deflection angle	
φ	azimuthal angles	
θ_1	incident trajectory angle	
θ_2	transmitted trajectory angle	

-

-

-

LIST OF FIGURES

LIST OF TABLES

PAGE

:

ABSTRACT

Laser has got a property of having high irradiance and penetration power to be used for different medical purposes such as diagnostic, imaging, and treatment of several diseases. When laser interacts with tissue (considering particle nature of laser light), photons get absorbed, scattered or transmitted depending upon optical properties of the tissue. For laser treatment, information such as fluence rate, reflectance, power, spot size etc. should be known a priori. The optical properties of tissue affect the photon distribution inside the tissue. Therefore, Monte Carlo method is used to simulate photon distribution. The effect of variation of scattering coefficient, anisotropy, and refractive index of tissue (optical properties) on fluence rate and reflectance is studied. The scattering coefficient variation shows changes in fluence rate, in which penetration of photon is high for lower scattering coefficient and decreases as the coefficient increases. Photons get evenly distributed for lower value of anisotropy of the tissue. Parametric studies suggested that refractive index did not have significant effect on the fluence rate and the reflectance.

Keywords: photon distribution, optical parameters, Monte Carlo simulation.

CHAPTER 1
INTRODUCTION

1.1 Historical Review

Laser an acronym for Light Amplification by Stimulated Emission of Radiation is a device which emits light through a process of optical amplification based on stimulated emission of photons. The emitted laser light has got high degree of spatial and temporal coherence which is unattainable using other sources. Laser beam can be focused to a very tiny spots thereby achieving very high irradiance or they can be used as a beam of low divergence in order to concentrate their power at a large distance. As the technology evolved, different types of laser were invented which were used for different purposes. They included gas laser, chemical laser, dye laser, metal-vapor laser, solid-state laser, semi-conductor laser and free electron laser. Some types of laser were used in field of medicine where its irradiance properties were highlighted for treatment of various diseases. It was used in many disciplines of medical treatment such as dentistry, dermatology, orthopedics, retinal disorders, Optical Coherence Tomography, forensics optics, light simulation of nerves etc. For any therapeutic treatment parameters responsible are power, irradiation time, spot size for continuous wave lasers and energy per pulse, irradiation time, spot size, repetition rate, and number of pulses for pulsed laser. Lower irradiance are associated with diagnostic application as it does not increase temperature while high irradiance are capable of ablating tissue, inducing plasma formation, and creating mechanical damage in tissue. The depth of laser light penetration in the tissue depends upon its optical properties which vary with wavelength [1].

Tissue is cellular organizational level intermediate between a complete organism. It is an ensemble of cells not necessarily identical, but from same origin, that together carry out

identical functioning. In laser tissue interaction tissue are treated as an absorbing and scattering medium. Owing to the interaction with light it shows optical and thermal effects. Optical properties are estimated by measuring reflectance and transmittance. Photon absorption can cause heating, which drive ionization, with changing the optical properties. This raises the absorption of the incident light causing further increase in heating, leading to cascade inducing plasma formation, eventual pressure rises, and expansion of the material [1].

For optimum treatment conditions physicians must select a laser, a beam power, a spot size and irradiation time. For modeling of any type of laser treatment –photochemical, thermal, or ablative, it is important to examine distribution of photon in the tissue. Light distribution in thermal and ablative effect is directly proportional to heat source. In photochemical application release of singlet oxygen is proportional to distribution of light. Since these treatments are depending on optical properties of laser, the light transport model used was approximate and heuristic. Assumption and approximation in the modeling of photon distribution should be avoided as it makes it worst for modeling. In Kubelka-Munk approximation that model light distribution assumes immediate surface to be isotropic, but light can undergo several scattering before reaching isotropic profile. The optical properties measured can only be used for Kubelka-Munk theory [2]. The method which exists is impractical for optical properties measurement as a function of wavelength, and is ill-suited [3-5]. Attempts made for measuring the phase function does not generate quantitative analysis and may not be used in more complex model [6, 7].

An exact assessment of laser propagation in tissue requires a model that characterizes the spatial distribution of photons in tissue structure, their absorbing properties, and refractive indices. This is effectively done by Monte Carlo simulation. Monte Carlo results are consistent with transport theory, which is an analytical theory for describing light propagation in turbid media. The power of the Monte Carlo methods lies in its ability to handle virtually any source, detector and tissue boundary conditions, as well as any combination of tissue optical properties. However, it has the fundamental limitation that the optical parameter space is sampled at only one "point" (point of interaction) at a time, so that any single Monte Carlo simulation gives little insight into the functional relationships between measureable quantities and the optical properties. The Monte Carlo simulation describes light as particles propagating in a medium containing independent absorption and scattering centers. Finding the light energy that reaches a target chromophore per unit area per unit time at some position is the first task of modeling. In Monte Carlo simulation, large numbers of "photons" are launched at a location defined by *x, y, z* coordinates with a trajectory defined by directional cosines (projection of trajectory onto *x, y* and *z* axes). The random distance travelled before the photon interacts with the tissue is based upon the selection of a random number [0, 1] and the total attenuation coefficient of the medium. At the end of each photon step, the weight of the photon is reduced by absorption. The remaining non-absorbed weight is redirected according to a scattering (or "phase") function that describes the angular dependence of single scattering by the particular tissue. Once a new trajectory is specified, the photon is again moved a random distance [1].

1.2 Interaction of Light with Tissue

1.2.1 Introduction

The light when interacts with tissue, the photons is absorbed or remains unabsorbed within the tissue. The unabsorbed light either is transmitted, emerging from other side or else it gets re-emitted. When light is in the tissue, it may change its direction or continue to travel in its previous path. Light is assumed as a stream of photon, and particle theory of light explains the quantum nature when absorption of light increases the energy of the system. The interaction of light with tissue depends on the properties of incident light and optical properties of tissue, which controls the propagation [1].

Remission occurs when the light reflects from the front or scatters and passes through the interface leaving the tissue Scattering of light occurs when it interacts with the tissue (fluctuation in index of refraction) and changes direction, without changing the wavelength. Absorption of light in tissue induces changes in the energy state from ground to excited state which drives number of chemical processes.

1.2.2 Tissue Optics

Optics of laser irradiation of tissue is best defined by inspecting the response of a target photon inside the tissue. The optical characteristics of the tissue: absorption and scattering within the tissue, reflection and transmission at boundaries decides the number of photon that will reach inside the tissue. Frequent scattering takes place for each photon. Photon can be absorbed by tissue chromophore, besides scattering. Photon propagation in tissue is modeled that characterizes the spatial distribution.

Finding the light energy which reaches a target chromophore per unit area per unit time at some position (fluence rate) is often simulated with Monte Carlo method. Large number of photon is launched in tissue and paths are followed. It describes light as a particle which is propagating in a medium containing independent absorption and scattering centers.

1.2.3 Propagation of Light in Tissue

Propagation of Collimated light: A collimated laser beam normal to the surface with uniform irradiance has a small portion of light reflected through the surface and remaining light is attenuated in the tissue by absorption and scattering. The fluence rate along z direction is given by

$$E(z) = E_0(1 - r_{sc})e^{-(\mu_a+\mu_s)z}$$

Penetration depth: It is the mean free path for absorption or scattering event, where the percentage of collimated light beam in the tissue is reduced to 37%, given by equation

$$.E(\delta) = E_0(1 - r_{sc})e^{-1}$$

The collimated penetration depth is given by $\delta = 1/\mu_t$

Optical Depth: Optical thickness and physical thickness *d* are related by the equation

$$OD = \mu_t d$$

The transmission of collimated beam through a tissue of OD value 1 is 37 %.

1.3 Literature Review

Monte Carlo is a technique which was first proposed by Metropolis and Ulam [8] for simulating physical process using stochastic model. Monte Carlo method comprises of recording photon histories as it gets scattered and absorbed. Later, it was used to model photon distribution in tissue. An extreme example of sophisticated Monte Carlo simulation is MCNP code package [9]. The Monte Carlo simulation which is developed and used frequently neglected anisotropy and internal light reflection to model laser-tissue interactions [10]. The Adams and Wilson used Monte Carlo method for photon transport in biological material (1983), considering isotropic scattering [11]. Later, in 1987, Keitzer introduced anisotropic scattering for Monte Carlo simulation, implementing a simulation of biological tissue which propagates photon for cylindrical coordinates, using Hop/Drop/Spin nomenclature for program organization. This made the method useful which was in accordance with the tissue characteristics [12]. Photon propagation based on Cartesian coordinate was done by Prahl made the program much simpler to deliver information in written form by reformulating the program [13]. The work of Keitzer and Prahl was augmented by Wang and Jacques (1993) which considered tissue as multi-planer layer having different optical properties for each layer, and subsequently adopted a Monte Carlo Multi-Layered (MCML) program [14]. The MCML code is a well-organized program which employs simple input text and can be modified by the user for different specific problem, allowing various problems to be run without the need of recompiling each time. It has been widely spread through the web as source code, modified by various groups for dealing with variety of problems [15, 16]. Wang and Zhang [17] simulated the photon process in human brain and skin tissue with various sources and detector separation

distances using Monte Carlo simulation method. The human brain model and the skin model that were used had five layers and seven layers, respectively. In 1998 Jacques reported the use of Monte Carlo in specifying the point spread function for light in planar, spherical, and cylindrical coordinates in tissue from plane, line and point source respectively, by using minimal Monte Carlo program called mc321.c [18, 19]. Several modifications were done by students for their own specified objective [20, 21]. A Monte Carlo subroutine was prepared by Jacques (2003) that allowed routine calls to Monte Carlo, with updated versions. The mc321.c was modified for simulating polarized light transport using stokes vector state [22, 23]. Andrew and groups developed a distributed Monte Carlo stimulation which modeled the propagation of light through tissue. It allowed the improved calibration of medical imaging devices for investigating tissue oxygenation in the white matter of the cerebral cortex.

Since photon distribution is an important aspect of laser interaction with tissue, the main objective is to simulate photon distribution and to study the effect of optical parameters on the fluence rate and reflectance using Monte Carlo simulation.

CHAPTER 2

MATHEMATICAL MODELING

2.1 Model Description

2.1.1 Introduction: For modeling of light transport in tissue Monte Carlo Simulation is used which is very versatile and effective. Diffusion theory, a fast and convenient method to model light transport fails when there is gradient of fluence rate which is not linear. The shortcoming is overcome by Monte Carlo simulation. A general Monte Carlo method launches photons in tissue at a location (x, y, z) with a trajectory defined by direction cosines. The distance travelled by photon randomly within the tissue depends on random number selection and total attenuation coefficient of the medium before it interacts with the tissue. Weight of photon is reduced due to absorption at each photon step. The non-absorbed photon weight with the dependence on scattering function is redirected. When a new trajectory is quantified again the photon moves a distance randomly. The photon path, reflection, scattering, refraction play an important role in distribution profile. Monte Carlo modeling is used for a wide range of problem where sampling of probability density function is done [2].

2.1.2 Sampling*:* For Monte Carlo simulation of light propagation in tissue random selection of photon step size, scattering angle, reflection or transmission is required at the boundaries which is accomplished by random number in the range of [0,1] assigned to a random variable *x*. Density function *p(x)*and distribution function *F(x)*is used to establish a relation.

$$F(x_1) = \int_0^{x_1} p(x)dx = function(x_1)$$

This equation is used to relate *p(x)*, value of distribution function at a particular value x_1 of the random variable x which is equated with a random number RND in the interval [0, 1].

$$RND_1 = F(x_1)$$

This expression allows a series of values RND_1 for specification of series of x_1 values. The histogram of x_1 values will conform to probability distribution function *p(x).*

2.1.3 Step Size of Photon: Prediction of photon step size between interactions events is done by the sampling method. A photon which moves a step size is exponentially distributed and its value is dependent on the total attenuation coefficient which is equal to summation of absorption and scattering coefficient, ($\mu_a + \mu_s$). Photon's mean free path length is $1/\mu_t$ before it get absorbed or scattered. To specify the probability density function the first step size is used to describe the probability of a particular photon step sizes:

$$p(s) = \frac{e^{(-\mu_t s)}}{\mu_t}$$

Were $$\int_0^\infty p(s)ds = \int_0^\infty \frac{e^{-\mu_t s}}{\mu_t}\, ds = 1$$

The next step is to describe the integral of *p(s)* at a particular s_1 defining the probability distribution function

$$F(s) = \int_0^{s_1} p(s)ds = \int_0^{s_1} \frac{e^{-\mu_t s}}{\mu_t} ds = 1 - e^{-\mu_t s_1}$$

Following step is to equate random number RND1 to the function *F(x)*, Solving for s_1, we get

$$s_1 = -\ln(1 - RND_1)/\mu_t = -\ln RND_1/\mu_t$$

Because of the uniform distribution of the random number between [0, 1] the term (1-RND_1) and RND_1 are equal. A series of step size is generated by a series of random number that follow the probability density.

Steady State Monte Carlo Propagation of Photons in Tissue*:* With the term steady state it is clear that there is a single distribution of light and no time dynamics comes into picture. For steady state Monte Carlo simulation it is convenient to consider distribution of photon as yielding the fractional density of incident light absorbed, when one unit of power or energy is delivered. By scaling A by the beam power P or radiant energy Q, the corresponding heat source matrix or radiant energy density matrix is obtained, such that

$$S=PA \text{ or } W= QA$$

The escaping flux density track is also kept in simulation out of the front surface R_r which is delivered with light, and out of rear surface T_r. Converting A into fractional transport within the tissue give fluence (φ) and fluence rate (ψ) by the following equations

$$\varphi_r = PT_r$$

$$\psi_r = QT_r$$

2.2 Computational Approach

The parameter required for Monte Carlo simulation is passed to the program. A simple semi-infinite homogeneous tissue is assumed. Parameters specified are absorption coefficient of tissue, scattering coefficient of tissue, anisotropy factor, and refractive index of tissue.

3D movement of photon is tracked by simulation over semi-infinite range. For boundaries specification parameters required are thickness of the tissues slab, refractive index of external medium outside front of tissue, refractive index of external medium outside rear of tissue.

The front surface is assigned with z=0, and rear with z=D. The history of photon is recorded, as the program run. Once a photon is absorbed its position is recorded as z. Number of photon to be delivered is specified. Typically 10^4-10^8 are launched depending upon the computation time available or required. Each photon takes step size of $1/(\mu_a + \mu_s)$ will drop weight at each step by a fraction $\mu_s/(\mu_a + \mu_s)$referred to as albedo. Initial weight of one is launched and it continues to propagate until it reaches a threshold. Number of steps and time required to reaches threshold conditions given by the expression

$$THRESHOLD = \mu_s/(\,(\mu_s + \mu_a)^{N_{steps}} \quad \text{and}$$

Number of steps is $N_{steps} = \ln(THRESHOLD)\,/\,\ln(\mu_s/\,(\mu_s + \mu_a)\,)$

The value of anisotropy factor and refractive index does not have any effect on the number of steps, therefore the time required to run $N_{photons}$is

$$t = N_{photons}\, t_{per\ step}\, N_{steps}$$

Photon with an initial weight of one is launched. The weight is decremented as the photon propagates. The weight deposited and weight escaped as transmittance or reflectance is normalized when a large number of photon are launched. The results are expressed as the fraction of photon absorbed, transmitted or reflected. For collimated beam, photons are launched perpendicular to the tissue and enters the tissue at (0, 0, 0), their trajectory being

$$x = 0$$

$$y = 0$$

$$z = 0$$

and

$$ux = 0$$

$$uy = 0$$

$$uz = 1$$

The beam is a flat field beam with uniform irradiance beam having a radius a.

Photon launched along a trajectory takes a step along it. The step size is determined as

$$s = -\ln(RND)\,/\mu_t$$

Photon position is updated using the following equation

$$x = x + s\,u$$

$$y = y + s\,uy$$

$$z = z + s\,uz$$

As the photon attempts to move beyond the boundary escaping, while moving towards the front surface, it might get reflected by the surface boundaries due to difference in refractive index at the interface. Some photon is allowed to escape and rests are allowed to propagate inside the tissue. If the photon escape (z<0) a partial step is taken that will just reach the boundary surface, size of partial step denoted by s_1 is

$$s_1 = abs\,(\frac{z}{uz})$$

The photon weight reflected at the boundary is given by $w=R_1w$, R_1 denoting the internal reflection calculated using Fresnel reflection equation

$$R = \frac{((sin\theta_1 cos\theta_2 - cos\theta_1 sin\theta_2)^2)}{2}$$

$$\times \frac{((cos\theta_1 cos\theta_2 + sin\theta_1 sin\theta_2)^2 + (\,cos\theta_1 cos\theta_2 - sin\theta_1 sin\theta_2)^2)}{((sin\theta_1 cos\theta_2 + cos\theta_1\, sin\theta_2\,)^2 + (cos\theta_1 cos\theta_2 + sin\theta_1\, sin\theta_2)^2)}$$

The parameters responsible for internal reflection are refractive index of incident medium, refractive index of transmitted medium. The parameters in Fresnel equation is denoted as

$$\cos \theta_1 = uz$$

$$\sin \theta_1 = (1 - uz^2)1/2$$

$$\sin \theta_2 = \sin \theta_1 (n_1 / n_2)$$

$$\cos \theta_2 = (1 - \sin \theta_2)1/2$$

Photon position is updated by taking remaining portion of original step $s - s_1$, given by

$$y = (s - s_1)ux$$
$$y = (s - s_1)uy$$
$$z = (s - s_1)uz$$

When photon has arrived at a new position it interacts with the tissue, a fraction of photon weight μ_a/μ_t is absorbed and the rest μ_s/μ_t is scattered continuing the propagation. The new trajectory of photon is formulated by sampling the probabilities for deflection (θ) and azimuthal (φ) angles, where they are considered independently.

$$p(\theta) = \frac{1}{2}\left(\frac{1 - g^2}{(1 + g^2 - 2g\cos\theta)^{\frac{3}{2}}}\right)$$

which has the properties

$$\int_0^{\pi} p(\theta) 2\pi \sin\theta \, d\theta = 1$$

$$\int_0^{\pi} p(\theta) cos\theta \; 2\pi \; sin\theta \; d\theta = g$$

HG function is specified by

$$cos\theta = \frac{1 + g^2 - \left(\left(\frac{1 - g^2}{(1 - g + 2g \; RND)}\right)\right)^2}{2g}$$

For g=0, $cos\theta = 2RND - 1$ and for g=1, $cos\theta = 1$

Azimuthal angle is calculated using equation

$$\varphi = 2\pi \; RND$$

The trajectory of photon are updated based on the following equations

$$sin\theta = \sqrt{1 - \; cos\theta^2}$$

$$temp = \; \sqrt{(1 - uz^2)}$$

$$uxx = \frac{sin\theta(ux \; uz \; cos\varphi - uy \; sin\varphi)}{temp} + ux \; cos\theta$$

$$uyy = \frac{sin\theta(\; uy \; uz \; cos\varphi + ux \; sin \; \varphi)}{temp} + ux \; cos\theta$$

$$uzz = -sin\theta\ cos\theta\varphi\ temp + uz\ cos\theta$$

Finally the trajectory is updated by the following equations

$$ux = uxx$$

$$uy = uyy$$

$$uz = uzz$$

The photon continues losing its weight as it gets propagated inside the tissue and become progressively small. To terminate the photon Roulette method is used in which a threshold is chosen. A random number is generated and compared. If its value satisfies the condition its value is increased or else is terminated. When a photon is terminated a new photon is launched only if the total number of photons launched has not reached the maximum value.

CHAPTER 3
RESULTS AND DISCUSSIONS

Photons were launched along the axial direction. The total number of photon launched was 10^6. The optical parameters of tissue, viz., scattering coefficient, anisotropy factor, and refractive index, were varied. Throughout the simulation the value of absorption coefficient were kept constant. Random number test were performed to test the efficiency of the random number generator. Distributions of photon weight were analyzed with different values of scattering coefficient. Effect of scattering coefficient, refractive index, and anisotropy of the tissue on fluence rate and reflectance was studied. It has been found that refractive index of the tissue has insignificant effect on fluence rate and reflectance.

3.1 Random Number Test

Monte Carlo simulation requires generation of random numbers which are uniformly distributed. The generated random number should meet the required condition and should be efficient. The effectiveness of the random number generator is checked by comparing the value of π. The value of π is obtained as follows: the area of a circle quadrant inscribed in a unit square is obtained with the help of two random numbers representing x and y (x= RND_1, y= RND_2) such that $RND_1^2 + RND_2^2 \leq 1$. The pair (x, y) which satisfied the above condition is counted as hit. The fraction of hit is compared with the area of circle quadrant, i.e. $\pi r^2/4$=hit/N, where N is the total number of pair of random number, which ultimately gives us the value of π.

Different numbers of pair of random number (N) were used and percentage error was calculated and tabulated in Table 1. It was found that the value of π calculated using random number was approximately equal to the actual value of π for N equals to 10^6 or 10^5

with least % error among three different numbers. Thus the method of random number generation was efficient.

Table1: Percentage error in value of π

N	π	%Error
10^4	3.1370	0.146
10^5	3.14392	- 0.074
10^6	3.13918	0.076

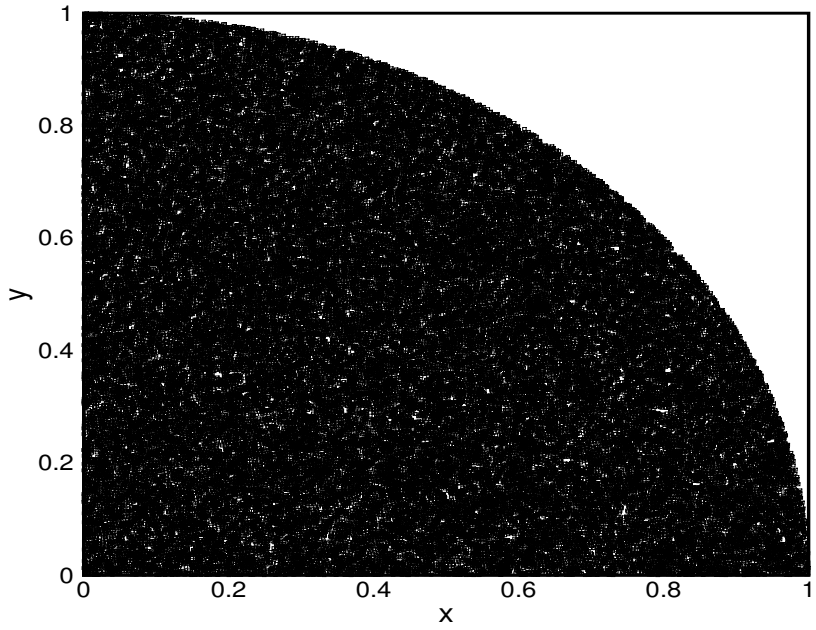

Figure1 : Effectiveness of random number generator

Figure 1 shows the black portion as hit. There are still some white spots seen in the black region, which is because of the number of photons. If the random number pairs are further

increased the white spot is likely to be filled with photon hit, covering the entire circular area.

3.2 Distribution of Photon Weight

For simulation photons were launched along the axial direction, which on propagating inside the tissue undergo reflection, remission and absorption due to interaction with tissue. The fraction of photon which escaped, reflected, and absorbed in the tissue did change but the net weight of the photons entering and leaving the tissue remain constant throughout the process which can be noticed in Table 2.

Table 2: Distribution of photon weight for varying scattering coefficients

μ_s [cm^{-1}]	Specular Reflectance	Escaped Weight	Absorbed Weight
50	0.0277777778	0.261434277	0.710788059
100	0.0277777778	0.377757084	0.594465198
200	0.0277777778	0.494966199	0.477256045

The variation in specular reflectance, escaped weight, and absorbed weight shows that for higher scattering coefficient, the escaped weight is higher since it scatters the photons with more intensity and as the value decreases the photons get more opportunity to enter the tissue and penetrate deeper inside it.

3.3 Fluence Rate Variation

Fluence rate is determined for different values of μ_s, n_2, g to study their effect keeping absorption coefficient constant. Different values of parameters considered are: g= 0.7, 0.8, 0.9 and μ_s = 50,100, 200. Figures 2 to Figure 7 represent the variation of fluence rate for the studied parameters.

3.3.1 With Different Values of Scattering Coefficient

The contours of fluence rate for different values of scattering coefficient, viz., 50, 100, and 200, are shown in figure 2-4. When scattering coefficient is varied a prominent difference in the pattern of fluence rate is noticed. The photon scatters less and penetrates much deeper for lower value of scattering coefficient as because they get opportunity to move a longer distance with greater step size before it interacts with the tissue at a new position. As the value of scattering coefficient increases, the scattering increases and photon experiences frequent scattering with smaller step size which results in more circular profile of fluence rate. For lower scattering coefficient the photon penetrates much deeper with intensity decreasing outward the radial distance. The uneven interface of different region is likely to go if the number of photon is increased.

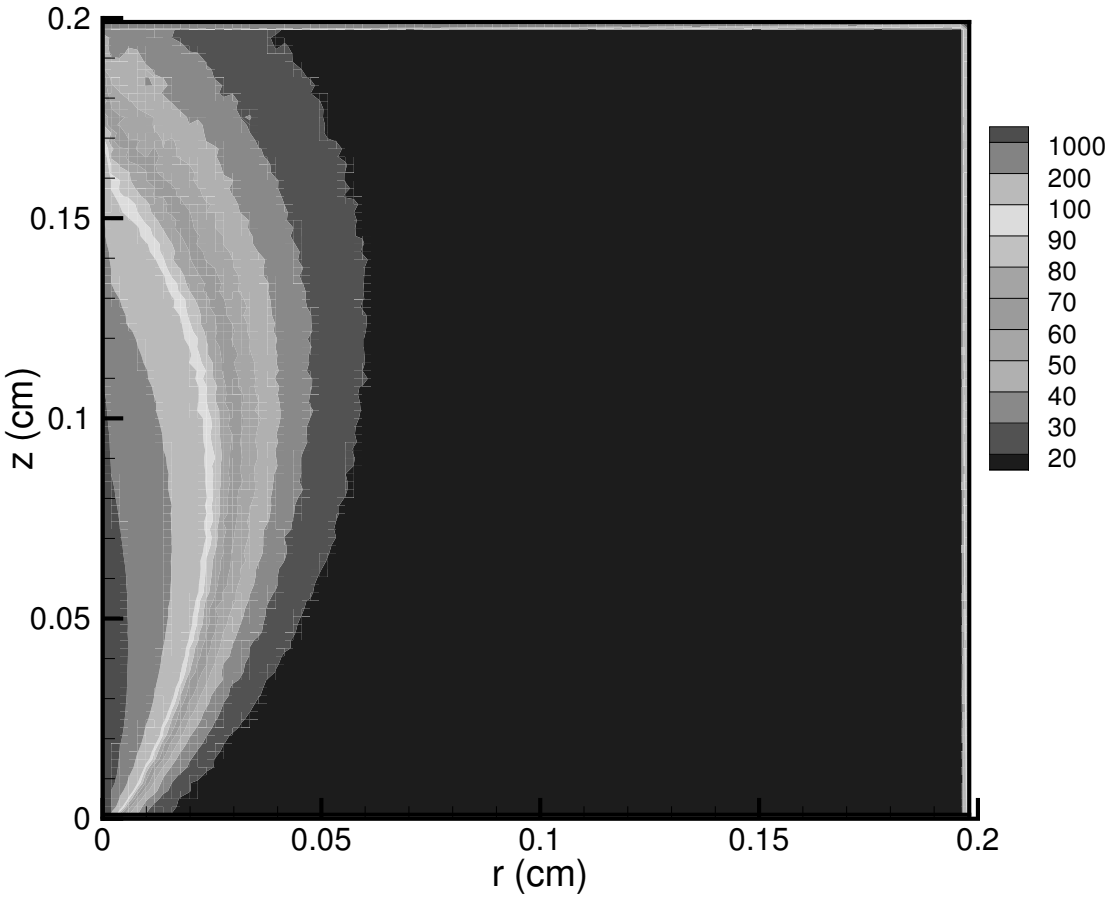

Figure 2: Variation of fluence rate in tissue for scattering coefficient 50 cm $^{-1}$

The scattering coefficient decides the fate of each photon which is entering a tissue. For scattering coefficient 50cm^{-1} (Figure 2) the scattering experienced by the photon is less and therefore the photon gets a fairer chance to penetrate inside the tissue much deeper along the axial direction.

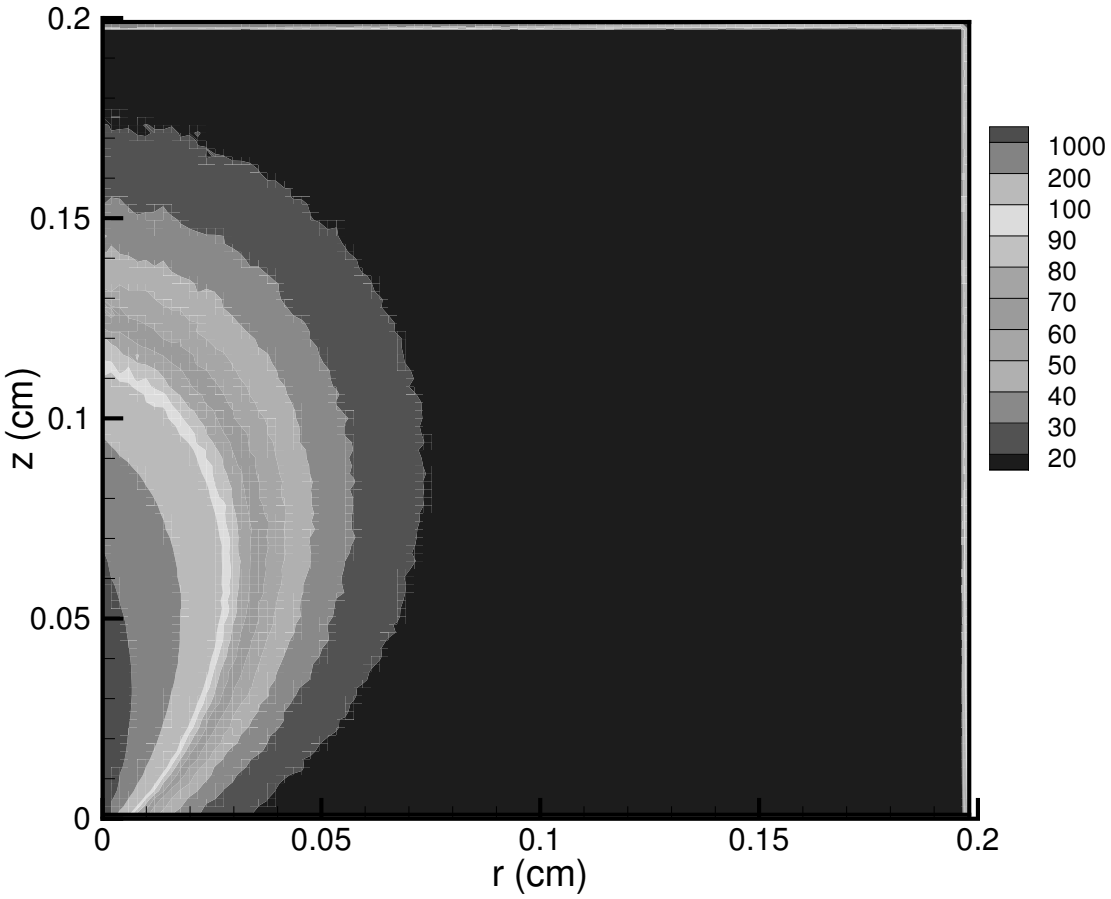

Figure 3: Variation of fluence rate in tissue for scattering coefficient 100 cm $^{-1}$

When the value of scattering coefficient is increased to 100cm^{-1}, it is clearly noticeable that scattering is increased (Figure3). The photons scatter more and are not able to move longer distance along the axial direction, showing less penetration. Since scattering coefficient is more photon manages to travel and penetrate along the radial direction more than the previous case

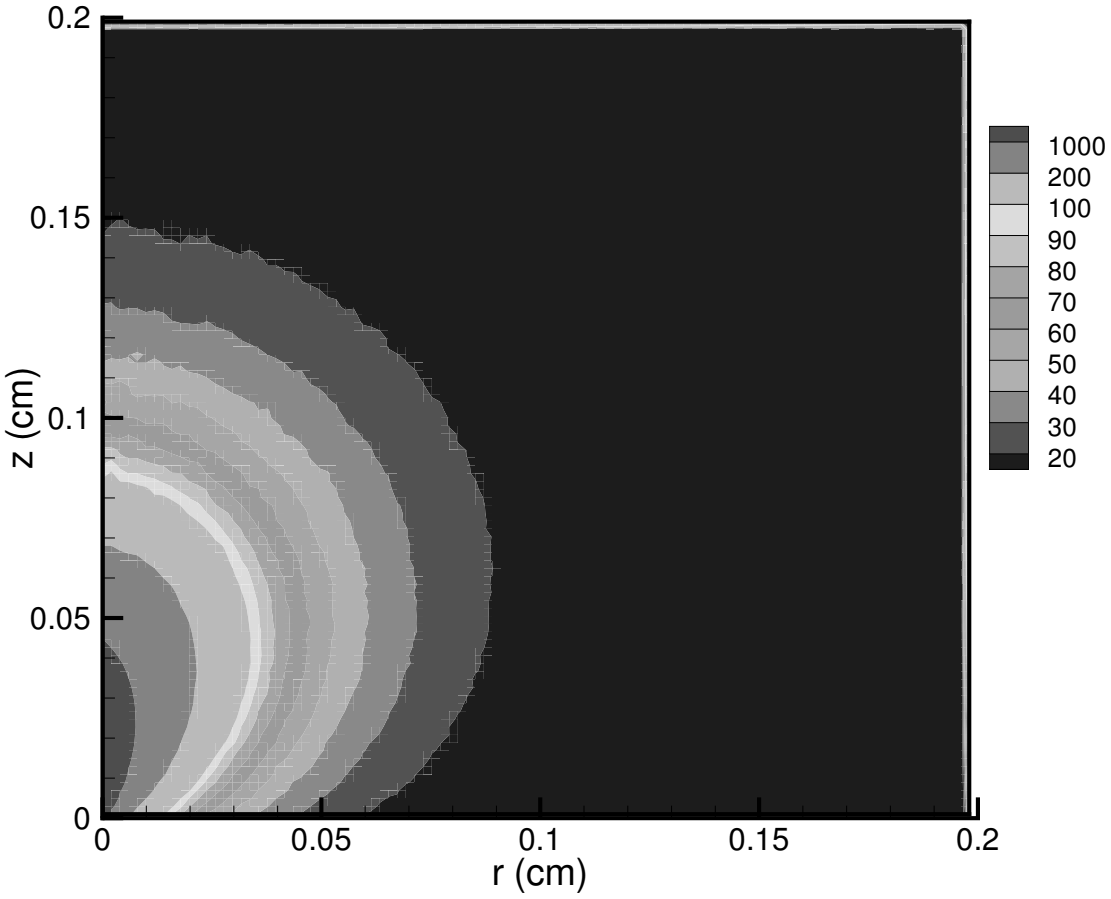

Figure 4: Variation of fluence rate in tissue for scattering coefficient 200 cm^{-1}

Further increase in scattering coefficient to 200 cm^{-1}decreases the penetration along the axial direction even more (Figure 4) and photon penetration along the radial direction increases covering more area radially than the previous cases. Photons suffer frequent and random scattering, which causes the photons to distribute evenly.

3.3.2 With Different Values of Anisotropy Factor

The contours of fluence rate for different values of anisotropy, viz., 0.7, 0.8, and 0.9, are shown in figure 5-7. When anisotropy is varied a prominent difference in the pattern of fluence rate is noticed. Photons distribution is isotropic for less value of anisotropy factor, irrespective of the scattering giving a semi-circular and symmetrical profile. With increasing anisotropy the fluence rate profile along the radial and axial direction approaches toward less semi-circular and unsymmetrical profile. This shows that it is losing its isotropic nature and is becoming anisotropic. The distribution of photon becomes prominent in one direction than the other.

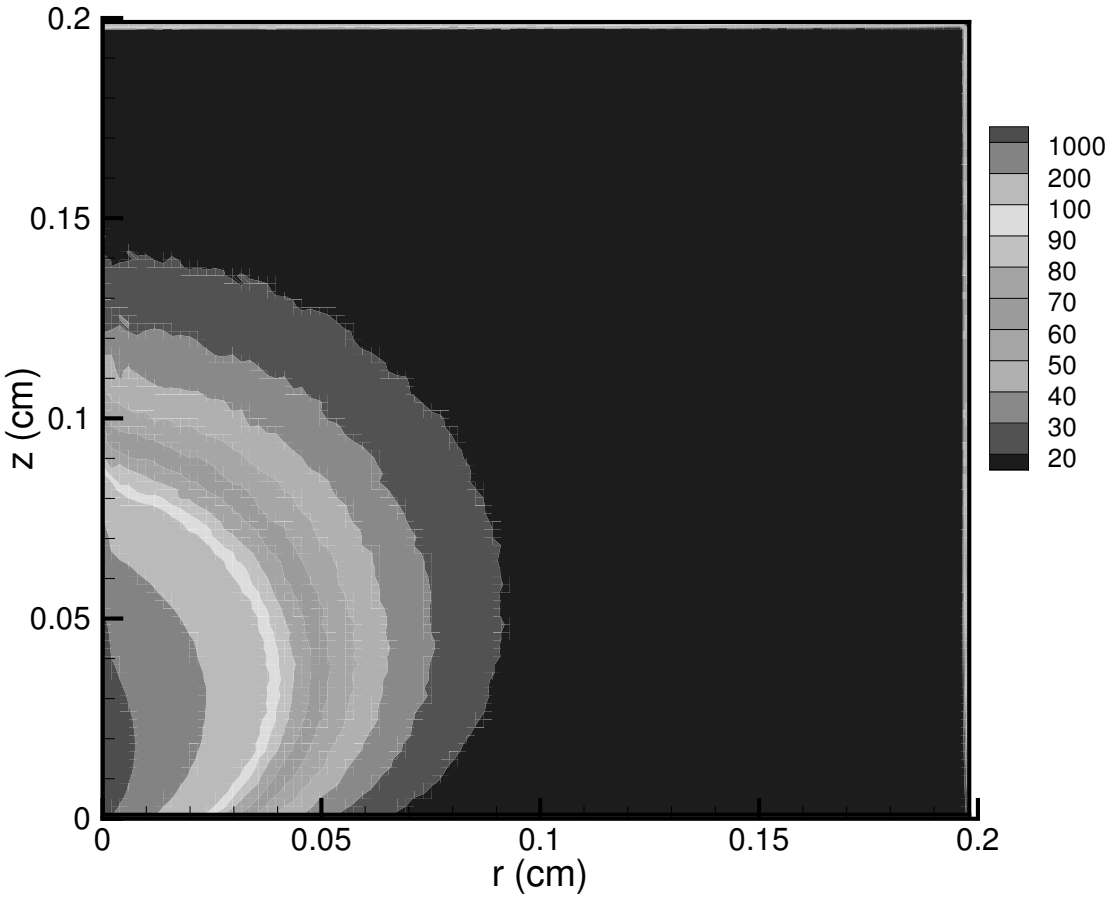

Figure 5: Variation of fluence rate in tissue for anisotropy = 0.7

For less value of anisotropy 0.7 (more isotopic) the profile is more likely approaching semi-circular profile (Figure 5), in other word is approaching toward isotropic condition. It allows the photons to distribute evenly in the tissue, which allows uniform distribution along any direction.

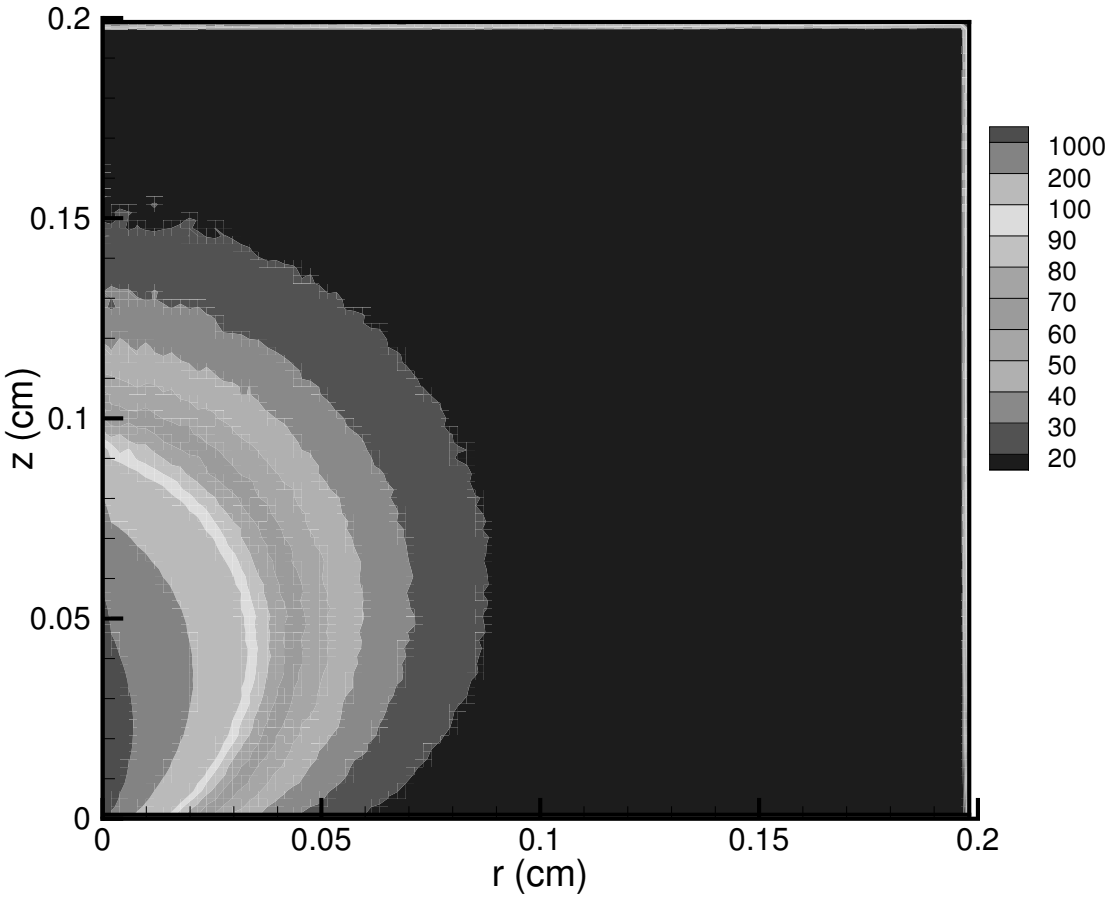

Figure 6: Variation of fluence rate in tissue for anisotropy = 0.8

As the anisotropy value increases to 0.8, the profile attain non semi-circular profile (Figure 6), distributing photon unevenly in the tissue. The penetration of photon is prominent in one direction, along axial direction.

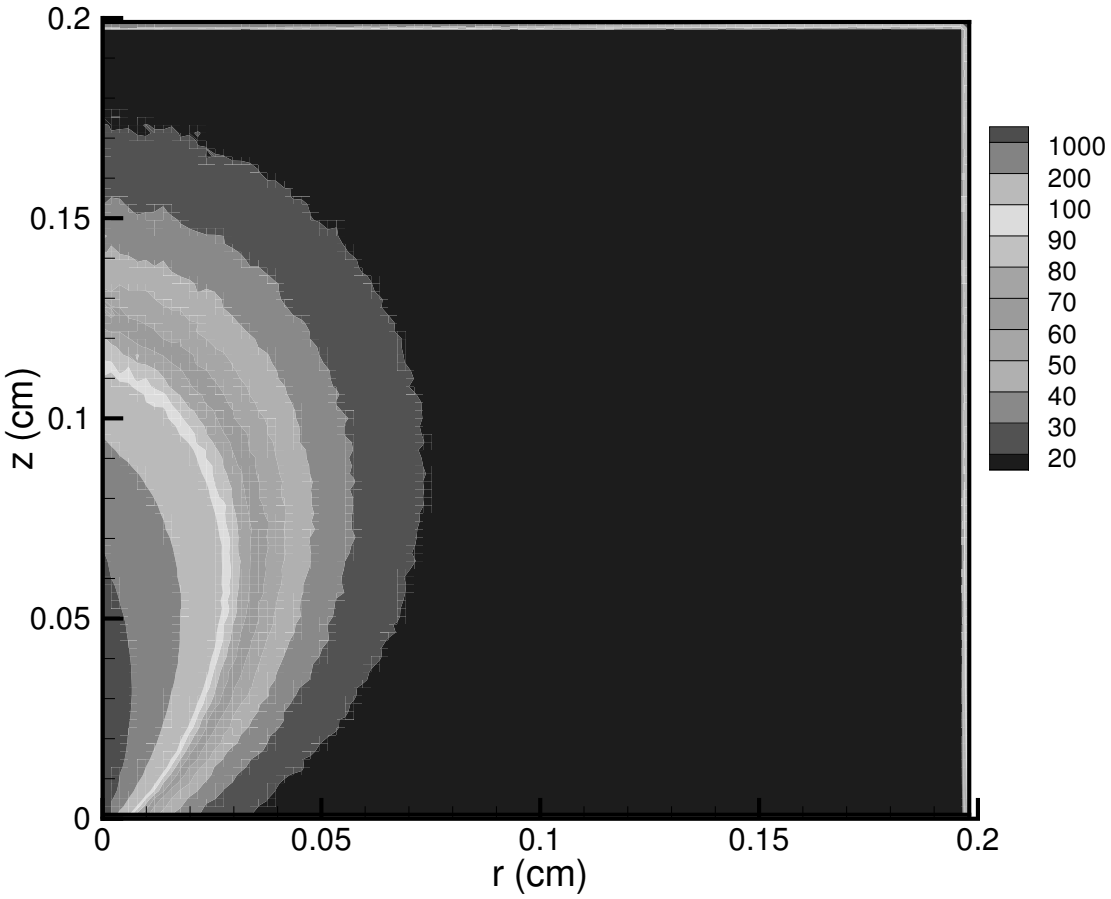

Figure 7: Variation of fluence rate in tissue for anisotropy = 0.9

Further increase in anisotropy to 0.9 shows the distribution of photon even more uneven (Figure 7). The photon is penetrating the tissue along axial direction more than the radial direction. This causes non-uniform distribution of photons in the tissue.

3.4 Reflectance Variation: Reflectance is determined for different values of μ_s, n_2, g to study their effect keeping absorption coefficient constant. Different values of parameters considered are: g= 0.8, μ_s = 100, n_2 = 1.3, 1.4, and 1.5. Figures 8 to Figure 10 represent the variation of reflectance for the studied parameters.

3.4.1 With Different Values of Scattering Coefficient

For different values of scattering coefficient, without varying anisotropy factor and refractive index of the tissue, reflectance variation along the radial direction is examined. This shows increase of reflectance with increasing scattering coefficient. The value of reflectance is higher at the point of irradiance and it decreases towards the radial direction (Figure 8). The maximum value of reflectance is 370 $cm^{-1}s^{-1}$, 560 $cm^{-1}s^{-1}$, and 1200 $cm^{-1}s^{-1}$ for scattering coefficient 50cm^{-1}, 100cm^{-1}, and 200cm^{-1} respectively. Thus it is observed that the reflection of incident radiation is higher for high scattering coefficient. The photon density is higher at the origin because of which reflectance is higher at this point.

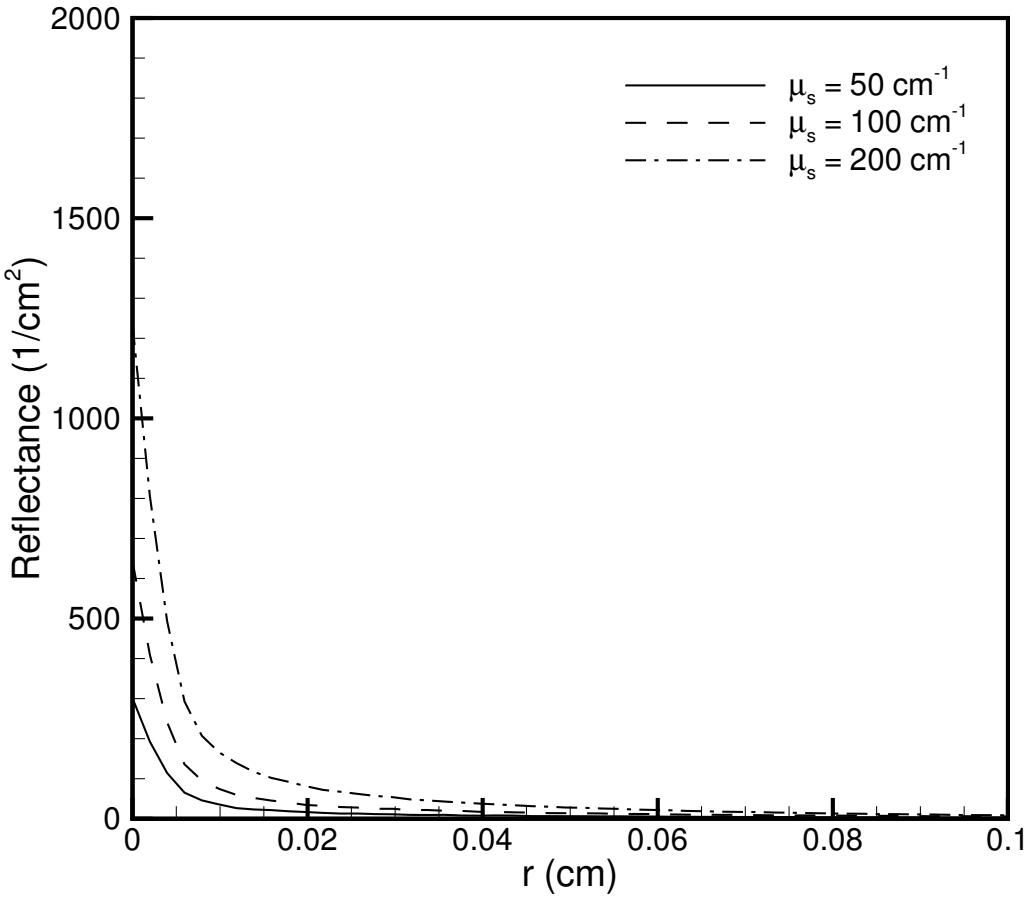

Figure 8: Variation of reflectance in tissue for different values of scattering coefficient

3.4.2 With Different Values of Anisotropy

For different values of anisotropy, without varying scattering coefficient and refractive index of the tissue, reflectance variation along the radial direction is examined. This shows increase of reflectance with increasing anisotropy factor. The value of reflectance is higher at the point of irradiance and it decreases towards the radial direction (Figure 9). The maximum value of reflectance is 600 $cm^{-1}s^{-1}$, 1200 $cm^{-1}s^{-1}$, and 1900 $cm^{-1}s^{-1}$ for anisotropy factor 0.7, 0.8, and 0.9 respectively. Thus it is observed that the reflection of incident radiation is higher for high anisotropy factor. The photon density is higher at the origin because of which reflectance is higher at this point. This shows that reflection of incident radiation is affected by the anisotropy. For even distribution of photon reflectance is higher as compared to the more anisotropic profile.

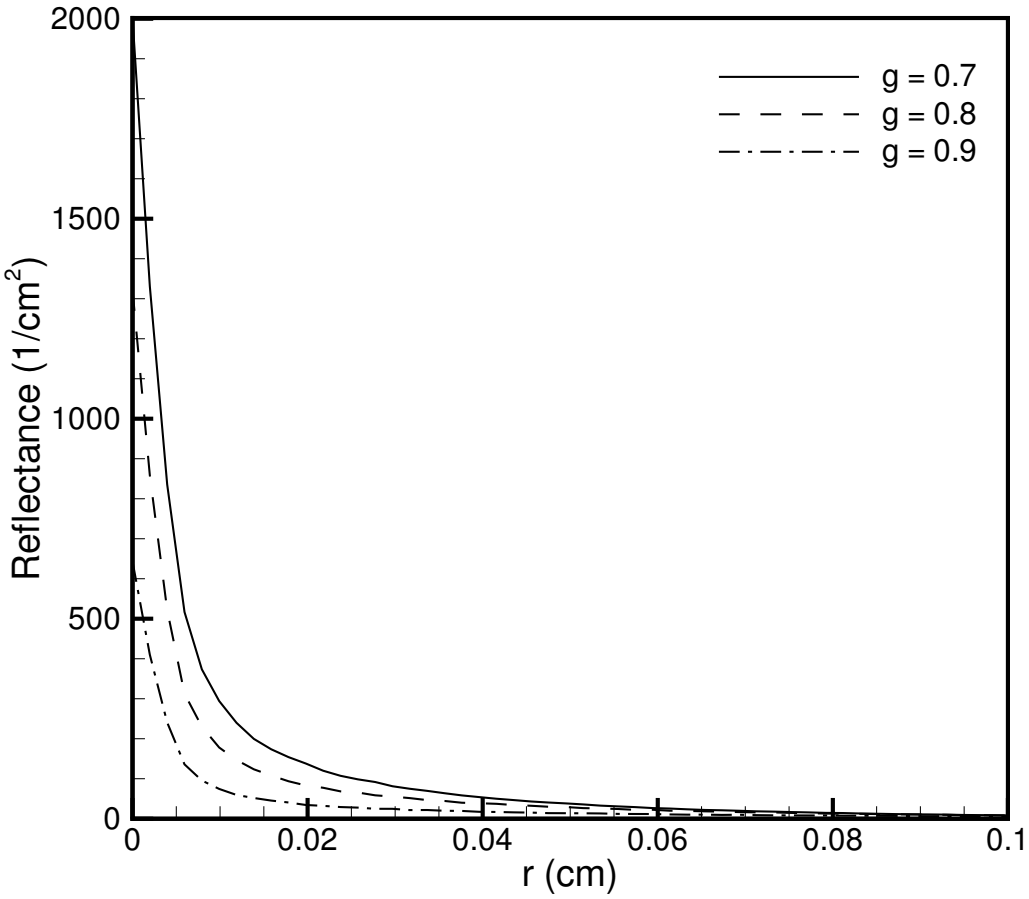

Figure 9: Variation of reflectance in tissue for different values anisotropy

3.4.3 With Different Values of Refractive Index of Tissue

For different values of refractive index, without varying scattering coefficient and anisotropy factor of the tissue, reflectance variation along the radial direction is examined. Since the tissue is assumed homogeneous, refractive index inside the tissue is uniform. The plot between reflectance and radial distance for different refractive index does not change much and shows deviation from the previous plot. The values of reflectance for different refractive index do not change and they coincide with each other (Figure 10). Variation in refractive index of tissue does not affect the value of reflectance along the radial and axial direction. Thus, it shows that reflectance is independent of refractive index of tissue.

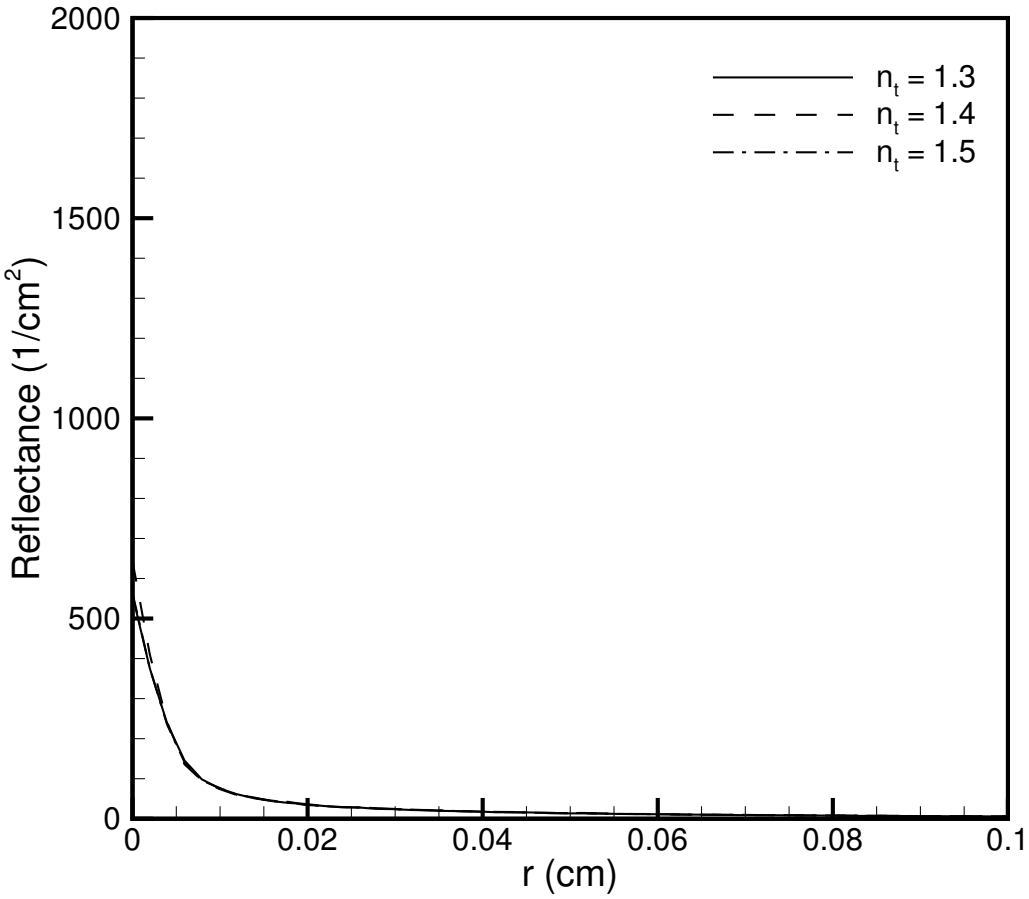

Figure 10: Variation of reflectance in tissue for different values of refractive index of tissue

CONCLUSION

The laser treatment in medical field has become popular. While interacting with tissue photons experience absorption and scattering, getting distributed in the tissue depending upon the optical parameters of tissue. The distribution of photon is simulated effectively by using Monte Carlo method. The variation of fluence rate and reflectance for different values of scattering coefficient, anisotropy factor, and refractive index is examined. The study showed that the photon distribution is affected by the tissue parameters. The penetration of photons is more along the axial direction for lower scattering coefficient and decreases with increasing values of scattering coefficient. For low anisotropy factor fluence rate is evenly distributed and becomes non uniform with increasing anisotropy. Reflectance increases with increase in scattering coefficient. The same is true for anisotropy factor; however, refractive index does not affect reflectance.

REFERENCE

1. Ashley J.Welch, Martin J.C. van Gemert "Optical –Thermal response of laser Irradiated Tissue", second edition.
2. S ,Prahl , 1988 "Light transport in tissue", (thesis),University of Texas,.
3. M. J. C. van Gemert and W. M. Star. 1987 "Relations between the Kubelka-Munk and the transport equation models for anisotropic scattering." Lasers Life Sci., 1:287-298.
4. G. Yoon, A. J. Welch, M. Motamedi, and M. C. J. Van Gemert. 1987 " Development and application of three-dimensional light distribution model for laser irradiated tissue." IEEE J. Quantum Electron., QE-23:1721-1733.
5. S. T. Flock, B. C. Wilson, and M. S. Patterson. 1988 "Hybrid Monte Carlo-dissusion theory modelling of light distributions in tissue." In M. W. Berns, editor, SPIE Proceedings of Laser Interaction with Tissue, volume 908, pages 20-28.
6. W. A. G. Bruls and J. C. van der Leun. 1984 "Forward scattering properties of human epidermal layers." Photochem. Photobiol., 40:231-242.
7. N. Metropolis and S. Ulam. , 1949 " The Monte Carlo method." J. Am. Statistical Association, 44:335-341.
8. R. A. Forester and T. N. K. Godfrey. "MCNP|A general Monte Carlo code for neutron and photon transport." In R. Alcou®e, R. Dautray, A. Forster,
9. G. Ledanois, and B. Mercier, editors, , 1983 "Methods and Applications in Neutronics, Photonics and Statistical Physics", pages 33{47. Springer-Verlag, New York

10.B. C. Wilson and G. Adam. 1983 “A Monte Carlo model for the absorption and °ux distributions of light in tissue.” Med. Phys., 10:824-830.

11. Schoonhove n R and Stegeman DF1991. “Models and analysis of compound nerve action potentials.”Crit. Rev. Biomed. Eng., 19:47–111.

12. Cole K. 1968 “Membranes, ions, and impulses: A chapter of classical biophysics.” Universityof California, Berke ly, p. 569.

13. Plonsey R and Barr R. Bioelectricity 2002 “A quantitative approach” Kluwer Academic, New York,2nd edition.

14. Hille B . 2001. “Ion channels of excitable membranes.” Sinaure Associates, Sunderland, MA, 3rd edition

15. Huang C , Harootunian A, Maher M, Quan C , Raj C, McCormack K, Numann R, Negulescu P, Gonzalez J. 2006“Characterization of voltage-gated sodium channel blockers by electrical stimulation and fluorescence detection of membrane potential.” Nat. Biotechnol ., 24:439–446.

16. McGill K, Cummins K, Dorfman L, Berlizot BB, Leutke meyer K, Nishimura D, Wi drow B. 1982 “On the nature and elimination of stimulus artifact in nerve signals evoked and recorded using surface electrodes.” IEEE Trans. Biomed. Eng ., 29:129–137.

17. Z.wang, L.Wang, Y.T.Zhang, X.D.Chen. “Monte Carlo Stimulation of light propagation in human tissue models.”

18. Civillico E and C ontreras D. 2005 "Comparison of responses to electrical stimulation and whisker deflection using two different voltage-sensitive dyes in mouse barrel cortex in Vivo." J. Membr. Biol ., 208:171–182

19. Palanker D, Vankov A, Huie P, and Baccus S. 2005 "Design of a high-resolution optoelectronic retinal prosthesis." J. Neural. E ng ., 2:S105–S120

20. Miller CA, Abbas PJ, and Brown CJ. 2000 "An improved method of reducing stimulus artifact in the electrically evoked whole-nerve potential." Ear Hear , 21:280–290.

21. Wu WH, Ponnudurai R, Katz J, Pott CB, Chilcoat R , Uncini A, R apoport S, Wade P, Mauro A. 1987 "A failure to confirm report of light-evoked response of peripheral nerve to low power helium-neon laser light stimulus." Brain Res ., 401:407–408.

22. Balaban P, E senaliev R , Karu T, Kutomkina E, Letokhov V, Oraevsky A, and Ovcharenko N. 1992 "He-Ne laser irradiation of single identified neurons." Lasers Surg. Med., 12:329–337

23. Bragard D, C hen AC, and Plaghki L. 1996. "Direct isolation of ultra-late (C-fibre) evoked brain potentials by CO2 laser stimulation of tiny cutaneous surface areas in man." Neurosci. Lett .,209:81–84